COMPUTATIONAL ELECTROMAGNETIC MODELLING OF A PROBE EMPLOYED IN PLANAR NEAR FIELD ANTENNA MEASUREMENTS

Lyon R.W., Gregson S.F., Mitchelson C., McCormick J.

BAE SYSTEMS UK

ABSTRACT

Over recent years the popularity of planar near field antenna measurement techniques has increased significantly. This is in part due to the ease and efficiency with which asymptotic far field parameters can be obtained from near field data using spectral techniques, and the removal of the requirement to displace the antenna under test during the sampling process. Crucially, in order that reliable far field patterns can be obtained from planar techniques, the plane wave receiving coefficients of the scanning probe must be taken into account during the transformation process. It is not usually possible to neglect these effects in a planar range because of the large angles of validity required and the short measurement distance employed.

Probe spectrum compensation requires an accurate knowledge of the propagating portion of the far field vector pattern function of the probe over the forward hemisphere. Generally, the best results are obtained from an auxiliary measurement of the probe, typically utilising a polar spherical geometry with as large a radius as is possible. However, the required plane wave receiving coefficients are not always available, as the characterisation process requires an *a-priori* knowledge of the required frequencies at which the probe is to be utilised. Unfortunately, the characterisation can prove expensive both in terms of facility time, cost and will inevitable require a degree of post processing in order that the very best results can be obtained.

Clearly, it would be attractive to obtain the plane wave receiving coefficients of the scanning probe directly from theory or from numerical simulation. This paper discusses the approach taken to obtain reliable far field parameters from Ansoft High Frequency Structure Simulator (HFSS), a commercially available finite element modelling tool that is not always considered when analysing electrically small antennas. Results are presented that illustrate the degree of agreement attained between numerical simulation and measurement obtained by using a quasi far-field polar spherical facility.

1. INTRODUCTION

One of the most significant contributions, albeit an extremely systematic one, to the overall error budget of conventional planar near field measurement technique results from inaccuracies in the characterisation of the near field probe. Conventionally, as the measured main-component pattern is proportional to the main-component probe pattern, errors in the corrected main polarisation pattern arising from probe characterisation errors will be a one-to-one mapping. That is, they have the same magnitude and direction as the errors in the probe pattern. The scanning probe consisted of a standard Orbit RF AL-2000-PRB-90 open-ended rectangular waveguide probe combined with a SWAM cone that was designed to minimise reflections from the mechanical interface located at the rear of the probe. A detailed description can be found below.

2. SPHERICAL MEASUREMENT TECHNIQUE

The monochromatic quasi far field electric vector pattern function was sampled in a temperature and humidity controlled screened anechoic chamber using a roll-over-azimuth geometry with an antenna under test (AUT) to probe separation, *i.e.* range length, of 12m. A polar spherical configuration was chosen in order that truncation, resulting from blockage from the robotics sub-system, could be minimised whilst ensuring that the crucial, rapidly varying near boresight cross polarisation pattern would be comfortably over-sampled.

In this configuration, the radius, r, is held constant and the angles θ and ϕ are varied with χ, *i.e.* polarisation, sequentially set to 0° and 90° to sample two orthogonal polarisation's thus resolving the propagating electric field onto a (polar) Ludwig II polarisation basis, *i.e.* E_θ, E_ϕ.

For data to be taken over the entire forward hemisphere the spherical angles were allowed to vary over the range, $-90° \le \theta \le 90°$ and $-180° \le \phi \le 180°$ such that inclusion of negative polar angles enables the pattern to be tabulated twice, once over the forward hemisphere and again over the alternative forward hemisphere. As the pattern of the instrument under test is time invariant differences between the respective patterns can be used to estimate the extent to which chamber multiple reflections were influencing the measured performance.

The sampling interval was defined according to the general sampling criteria. Usually, the AUT is mounted so that the radius of its minimum sphere r_t is made as small as possible. The minimum sphere is a conceptual sphere that is centred about the origin of the measurement system and completely encloses the majority of the current sources, *i.e.* the AUT. The highest significant spherical wave mode present in the test antenna field is usually taken to be (1),

$$N = k_0 r_t + 10 \qquad (1)$$

Here, r_t is in meters and k_0 is the wave number. The maximum permissible sampling increment in θ and ϕ is related to the highest significant wave mode through (1) is,

$$\Delta\theta = \Delta\phi \leq \frac{2\pi}{(2N+1)} \qquad (2)$$

Here, the radius of minimum sphere was measured directly and found to be approximately 30 cm. This length included the waveguide section and the majority of the SWAM cone. Thus, for the measurement configuration employed here a sampling increment of $\Delta\theta = \Delta\ \phi = 2°$ amply satisfied the sampling theorem. The required angular accuracy of the positioning system is typically taken to correspond to one fiftieth of a wavelength over the circumference of the minimum sphere, *i.e.* approximately twenty five times smaller than the required angular increment shown above. This is readily attainable with computer controlled rotational positioner fitted with any one of a number of encoders.

Minimising the radius of the minimum sphere r_t has other benefits. Placing the AUT over the centre of rotation results in the antenna occupying only a small portion of the test zone during the measurement procedure. Assuming that that the remote source antenna is electrically small with a relatively low directivity it is possible to approximate the test antenna with an ideal Hertzian dipole antenna and avoid the requirement for probe pattern correction. The aperture of the waveguide probe was carefully positioned to coincide with the intersection of the θ- and ϕ-axes of the range so as to minimise the size of the test zone required to characterise this instrument.

The probe assembly consisted of a chamfered rectangular waveguide section and cone fabricated from a surface wave absorbing material (SWAM). The properties of the SWAM material are described below in section 3. The probe was displaced from the positioner to minimise the effects of scattering, as the front-to-back ratio of a typical waveguide in free space can be as little as 10 dB.

Phase stability, usually compromised by thermal drift, was improved by utilising a tie scan correction technique. Here, when a scan was completed for a given polarisation, a single cut was taken through the region of largest field intensity by scanning the axis that had previously stepped. By taking data over a region of space on two occasions drift within the recorded phase can be determined and corrected.

Although a single polarisation standard was used to sample the spherical $\underline{\hat{e}_\theta}$ $\underline{\hat{e}_\phi}$ field components channel balance correction was required as a second, stationary, antenna was used to sample the reference signal. As a polar spherical measurement system had been utilised an auxiliary channel balance measurement was not required since the crucial correction parameters could be extracted directly from the boresight scan.

For a polar pointing spherical measurement the boresight scan involves taking ϕ_N measurements of essentially the same parameter with only a rotation of the polarisation reference. This is repeated for each orthogonal polarisation, *i.e.* once when the principal polarisation of the probe was aligned to the *x*-axis and again with the principal polarisation of the probe aligned with the *y*-axis. The channel balance correction factor was determined from the weighted mean difference between the equivalent measurements.

The very low gain nature of this instrument will inevitably result in the facility walls being illuminated by a relatively large amount of power. Additionally, the characterisation of the waveguide probe was found to be further complicated by sensitivity to the configuration of absorber placed behind the instrument indicating the existence of large sidelobes in the rear hemisphere. Latterly, this was confirmed by simulation.

The forward hemisphere of the probe pattern was sampled twice, conventionally and again in the alternate hemisphere configuration that enabled a determination of the multipath level within the facility. The average multipath level for the $\underline{\theta}$ and $\underline{\phi}$ polarisation's were found to be encouraging at -52.36 dB and -51.43 dB respectively. This can be thought of as representing the average change in room effects between configurations and is sufficiently small that further pattern correction was felt to be unnecessary.

The far field, or Fraunhofer, region is typically assumed to begin when the distance *r* is at least as large as the Rayleigh distance *i.e.*,

$$r \geq \frac{2D^2}{\lambda} \qquad (3)$$

Here, *r* is the distance from the antenna, *D* is the largest overall dimension where $D>\lambda$ and λ is the wavelength. Thus, as the maximum dimension of the wave guide probe was 25.02[1] mm, when operating at 10 GHz, the far field should begin when the distance is greater than 41.7 mm. This implies that measurements made at 12m should yield results that constitute a very good approximation of the true far field pattern function, *i.e.* when $r \to \infty$.

The true far field can be obtained by utilising the fact that antenna radiation can always be expressed in terms of an expansion of spherical wave functions that satisfy Maxwell's equations. The spherical near field transformation computer code SNIFT version d by TICRA Engineering Consultants was used to transform the measured from a sphere of radius 12m to a sphere of infinite radius. The input probe was specified as a

[1] The *x*-band wave-guide probe had a width of 22.86 mm and a height of 10.16 mm.

Hertzian dipole as no probe pattern correction was required and electric near field pattern was sampled. Probe pattern correction was avoidable as the AUT subtended a small angle as seen from the remote source antenna. The near field data was transformed to the far field using SNIFTd-ROSCOE-SNIFTd, using 90 polar and 89 azimuthal spherical mode coefficients, *N* and *M* respectively, the Euler angles were used to specify the rotation of the spherical mode coefficients. A Hertzian dipole output probe was specified in order that the spherical electric field components were obtained. The polarisation basis was immediately changed to a Ludwig III definition and the resulting far field pattern and the results compared with the re-tabulated measured 12m data set. Generally, the agreement was found to be very encouraging.

The differences observed between the two patterns at large polar angles was an artefact that results from the fact that the measured pattern is not spatially band limited, *i.e.* the function does not tend to zero at the periphery of the sampling interval which in this case was limited to $\theta = 90°$. Such a discontinuity can only be represented reliably by utilising a very large number of spherical mode coefficients. However, the actual number of modes used within the transformation process was much less than this as it was determined from applying the sampling theorem and equated roughly to two samples per wavelength over the surface of the minimum sphere. This resulted in the series representation of spherical wave functions not converging and resulted in spherical mode leakage. This manifests itself by introducing spurious ripple over the entire pattern and an absence of signal at large angles. This is *not* a weakness of the transformation process and merle illustrates an inappropriate choice of sampling interval from a transformation perspective. Thus, in this case, error introduced by the modal expansion was found to be greater than the combined error introduced by the interpolation scheme and the inability to probe the instrument in the true far field.

3. THE MODELLING TECHNIQUE

The far field vector pattern function of this near field probe was modelled using the proprietary finite-element modelling package High Frequency Structure Simulator (HFSS) supplied by Ansoft. The probe was constructed from a 240 mm length of waveguide 16 parallel plate rectangular waveguide with a coaxial to waveguide transition used to launch the fundamental TE_{10} waveguide mode. The waveguide section was sufficiently long to insure that any higher order modes excited by the launch would be attenuated by the time they reached the aperture plane. The open end of the waveguide section was chamfered to a knife-edge with a 12° taper that was intended to reduce the scattering cross section of the end of the probe.

A cone of SWAM was attached to the outside of the probe that intersected with the waveguide approximately 80 mm from the aperture. This cone was designed to shield the probe mechanical interface plate, used to align and fix the probe to the *y*-axis probe carriage, and thus reduce the scattering cross-section of the overall assembly. This is crucial, as a proportion of the scattered energy would otherwise be reflected back into the test antenna. SWAM is a thin, flexible loaded elastomeric sheet material that can be used as a surface wave absorber and as a broadband absorber over limited range of large angles of incidence and is backed with a thin conductor. This material typically yields a minimum reflection loss of –6 dB over the broad frequency band of 6-16 GHz at normal incidence. However, for normal incidence the reflection loss rises to approximately –27 dB. The SWAM cone was modelled as a homogeneous absorber of thickness 1.4 mm with dielectric constant of approximately 10 and a small loss tangent formed into the shape of a right cone backed by a thin copper conductor centred about the axis of the waveguide section. Unfortunately, the electromagnetic properties of SWAM have been found to be variable both between batches and within individual single batch. Consequently, the effect that the SWAM material has on the performance of the near field probe can only be modelled approximately.

This arrangement was modelled in HFSS using symmetry in order that the size of the problem could be quartered. The radiation box surrounding the structure was meshed so that the maximum length of a tetrahedron edge was no greater than a sixth of a wavelength. This was found to be sufficient so that the accuracy of the predictions was insured whilst the duration of the simulations was minimised. The use of fewer tetrahedrons than this was found to introduce a spurious large amplitude ripple on the far field pattern. A right frustum just a little over a quarter of a wavelength from the structure was utilised as the radiation boundary as this minimised the volume of space over which the mesh had to be formed. The frustum was constructed from great many planar surfaces that guaranteed a uniform distribution of tetrahedrons throughout space whilst attempting to minimise the angle of incidence of a majority of the illuminating wave fronts. The waveguide section was modelled as a perfect copper conductor and the medium in which the probe was situated was taken to be air. A standard port was used to inject guided electromagnetic field energy into the model.

HFSS was used to solve for the far field Cartesian electric field components tabulated on a plaid monotonic equally spaced polar spherical grid in the far field for a discrete frequency. Although the bandwidth of the waveguide section was relatively large, the TE_{10} mode propagates from above 6.56 GHz and the TE_{21} mode propagates from 12.12 GHz for internal dimensions of 2.286 cm by 1.016 cm, the performance of the probe in practice is limited by the coaxial to waveguide transition. As such, the probe is limited to operating from approximately 8 GHz to 12

GHz. HFSS was used to generate far field patterns solving for each frequency individually. Other options were available that supplied data over a range of frequencies however in this case they were found to yield less satisfactory results to the top and bottom of the band.

Initially, the SWAM cone was omitted from the simulations since it was not thought that it would greatly affect the results. However, it was found that the absorbing cone changed the copolar performance of the probe for large angles, ±40° and dominated the cross-polar response which was particularly noticeable on the inter-cardinal great circle cuts. The SWAM cone also introduced a small amplitude high angular frequency rotationally symmetrical ripple on both to principal and cross-polar patterns that was, to a certain degree, present within the measured patterns.

4. COMPARISON OF FAR FIELD RESULTS

The vanishingly small cardinal cross-polar pattern function encountered within the theoretical prediction is unrealistic. In practice, mechanical imperfections included within the fabrication of the probe, *i.e.* the walls of the waveguide will not be perfectly orthogonal and the end section will not be perfectly smooth, and will bleed energy from the co-polar pattern that invariably dominate the performance of the probe at these angles. Typically, an auxiliary polarisation characterisation is performed with the intention of obtaining polarisation correction parameters that can be used to calibrate theoretical predictions, which principally modify the response of the probe in these regions.

A detailed comparison of the measured and quasi far field pattern for the inter-cardinal cuts can be found presented in the figure 1 and figure 2 below together with the eleven point boxcar mean average equivalent multipath level (EMPL) for the 9 GHz case, *i.e.* convoluted with a short pulse. Here, errors within the measurement and the theoretical model have been lumped together into a single error term, plotted as a "dash-dotted" line. A slightly higher EMPL was found to be present within the elevation plane and is probably attributable to the larger field intensities that illuminate the walls of the measurement facility in this plane. The very low EMPL is encouraging as this can be used to confirm both the modelling technique and the measurement process. The fact that the EMPL for the copolar and cross-polar patterns are roughly equal further reinforces the idea that the limit of the observation results from the backscatter error contained within the measured data set.

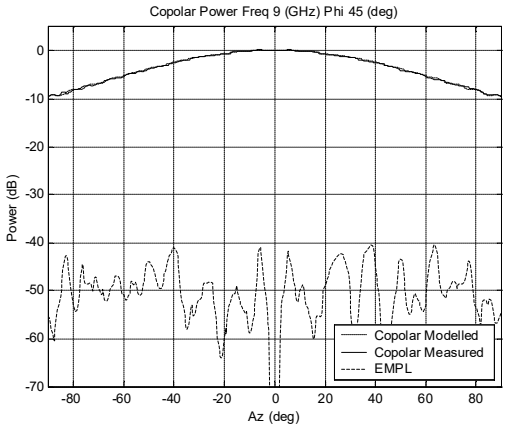

Figure 1: Far field inter-cardinal cut of copolar pattern.

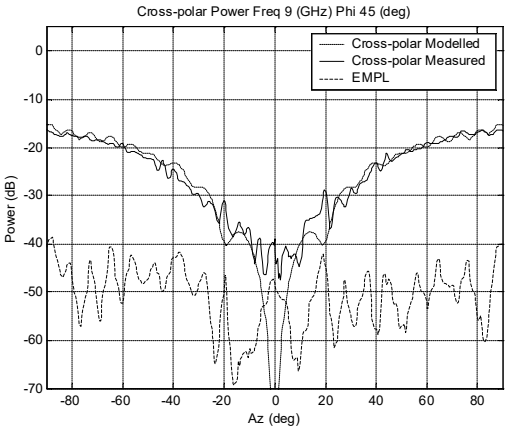

Figure 2: Far field inter-cardinal cut of cross-polar pattern.

For the case of conventional planar near field antenna measurements, errors within the characterisation of the probe pattern can be seen to correspond to errors in the measured pattern of an AUT in the form of a one-to-one mapping. Thus, planar measurements that have been taken using this probe and corrected using either the measured or modelled probe patterns can not be expected to have a relative amplitude pattern error with an EMPL of better than –50 dB. This model was used to predict the pattern at 1 GHz intervals over the frequency band of 8 GHz to 12 GHz. Crucially, a similarly encouraging degree of agreement was obtained over the entire band.

5. CONCLUSION

Good agreement has been obtained between numerical simulation and measurement thus verifying both the measurement and the use of the electromagnetic numerical simulation tool HFSS for problems involving the modelling of electrically small antennas. The modelling campaign has revealed that significant currents flow on the outside of waveguide probe that can significantly alter the cross-polar performance of the scanning probe.

REFERENCES

1. J.E. Hansen Editor 1988, "Spherical Near Field Antenna Measurements", Peter Peregrinus Ltd., London.